Journal of Loss Prevention in the Process Industries 72 (2021) 104565

Contents lists available at ScienceDirect

Journal of Loss Prevention in the Process Industries

journal homepage: www.elsevier.com/locate/jlp

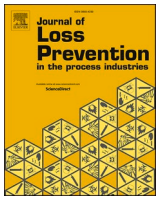

Behaviour of smoldering fires during periodic refilling of wood pellets into silos

Nieves Fernandez-Anez [a,*], Anita Katharina Meyer [a], Javier Elio [a,b], Gisle Kleppe [a], Bjarne Christian Hagen [a], Vidar Frette [a]

[a] Western Norway University of Applied Sciences, Bjørsonsgate 45, 5528, Haugesund, Norway
[b] Department of Planning, Aalborg University, 2450, Copenhagen, Denmark

ARTICLE INFO

Keywords:
Wood pellets
Silo
Smoldering
Cooling
Thermal runaway

ABSTRACT

The evolution of smoldering fires in biomass stored in lab-scale silos with additional fuel material supplied repeatedly, has been studied. The direct effects of the added material on the sample are: cooling, enhanced thermal insulation, and facilitation of more intense combustion at a later stage. This article focuses on the cooling, which leads to an almost instantaneous reduction in the combustion rate. Surprisingly, this reduction does not vary only with the amount of material refilled – but also depends strongly on the stage of the smoldering process. This demonstrates that the underlying smoldering processes merely to a certain degree are regularized by the periodic refillings. Quantitatively, the functional relationship between the refilled amount and the change in combustion rate caused by the refilling was determined. The results displays four regimes, that reflect different stages of the smoldering process at the time of the refilling. Using the Arrhenius equation, we find for one of these regimes an expression for the ratio of combustion rates (immediately after to immediately before the refill) as function of the amount of added material. This expression contains only one free (undetermined) parameter. We determine the value of this parameter from the data and demonstrate that this value is consistent with a simple model for how the sudden cooling occurs spatially in the sample.

1. Introduction

Biomass represents a way to harvest solar energy that is technologically simple. The use of biomass has continuously increased during the last 15 years and this rise is expected to continue. Within this group of fuels, forestry accounts for more than 60% of all EU domestic supply for energy purposes. In the EU, *wood pellets have become an important energy carrier traded on a large scale and over long distances, due to their high energy density and stable characteristics* (The European Commission's Knowledge Centre for The European Commission's Knowledge Centre for Bioeconomy, 2019). On the other hand, there are concerns that production of wood pellets directly from the main stems (instead of from wood wastes) may harm the climate (Searchinger et al., 2018). Irrespectively of the raw material used, large quantities of wood pellets are produced and need to be handled and stored. A common way of storing biomass is in vertical silos with roofs that prevent moisture absorption. With this configuration, large amount of material can be stored within a limited plant area.

Severe accidents in biomass production, storage, and transportation units, including explosions and large flaming fires, are often preceded by smoldering fires (Krause, 2009; Ogle et al., 2014; Russo et al., 2017). In turn, smoldering fires are typically ignited by weak heat sources, like malfunctional electrical or mechanical equipment. These are dangers that are easily underestimated and difficult to monitor. The same applies for the other main route to smoldering: self-heating (Babrauskas, 2003; Guo, 2013; Larsson et al., 2012). During self-heating, temperatures increase spontaneously in stored material of organic origin due to (exothermal) oxidation processes. Part of this heat accumulates in the material, accelerating the oxidation process, eventually leading to combustion of the material, a phenomenon known as self-ignition. While there have been many advances in the fundamental understanding of self-heating (which in most cases leads to smoldering), this scenario is still a challenge for users, like management of storage silos. The severity of the combined challenge from self-heating and malfunctional equipment was emphasized by a study that found – for a 16-year period – the number of accidents connected to the biomass industry to increase

* Corresponding author.
E-mail address: Nieves.Fernandez@hvl.no (N. Fernandez-Anez).

https://doi.org/10.1016/j.jlp.2021.104565
Received 27 November 2020; Received in revised form 28 May 2021; Accepted 4 June 2021
Available online 9 June 2021

faster than production (Moreno and Cozzani, 2015). Those authors found that the biomass supply chain and production of energy (electricity) from biomass dominated in the accident record, with fires as the most frequent outcome.

Consequences of smoldering in silos include loss of stored material, flaming fires, and dust explosions, causing both human and material losses. Detection of these fires before escalation is difficult, since they occur deep inside the material, release merely low quantities of gases, and reach only moderate temperatures (Lohrer et al., 2005). One experimental study, on an under-ventilated, laboratory-scale silo, found that low-intensity smoldering could exist without emitting any traces of carbon monoxide or carbon dioxide (Gentilhomme et al., 2019). The challenge is not only the weak signals (in terms of gases or temperatures), but the significant volume or area that must be monitored. In a recent contribution, a strong increase in emitted aerosols (particles or drops) was detected during slow heating of a sample – at temperatures well below the typical ignition temperature of smoldering. However, it is still not clear to which degree such a signal will be detectable outside a much larger volume, due to the filtering effect of cold regions in the material (Bluvshtein et al., 2020). Another promising direction is detection based on specific compounds (Madsen et al., 2018). However, techniques like these are far from ready for commercial implementation at large scale. Users and management of large storage and transportation units are often compelled to handle smoldering fires that went unnoticed until a late stage, for which no appropriate extinguishing techniques exist. Inert gases are expensive, and application does not necessarily lead to a satisfactory result. In particular, it has been argued that carbon dioxide should not be used due to danger for ignition of explosions. When pressurized carbon dioxide is released, small particles of solid carbon dioxide (dry ice) are formed in the gas stream, and these particles generate static electricity during their flight, which could constitute an ignition source (Hedlund, 2018). Attempts to extinguish these fires using water are often unsuccessful, even if significant amounts are applied. Water as extinguishing agent has at least two further drawbacks; runoff of contaminated water to surroundings, and significant expansion of pellets grains upon water absorption, with ensuing mechanical damage to installations like silos. The best solution in many situations is simply to let the contents of the silo burn.

The significant challenges for users and management of large storage and transportation units could be said to reflect the current level of fundamental understanding of smoldering; much is known, still more is unknown. Smoldering fires represent a slow, low-temperature, and flameless form of combustion that is very persistent and propagates through the fuel bed. Fuel materials that are prone to smoldering are typically porous, and thus have a large inner surface. This large inner surface is crucial, since the smoldering process involves direct reaction with oxygen at the surface of the solid material (Ohlemiller, 1985). Smoldering is encountered in a range of situations - from the built environment (buildings, furniture), via coal seams to wildlands (peat, forests). In all cases, there are major safety concerns, both directly from the fires as such, and indirectly from the huge, harmful emissions they generate (Rein, 2016). A recent, extensive review of smoldering research (Torero et al., 2020) attempts to bridge its two main directions: the fire-safety perspective, where uncontrolled and unwanted smoldering fires are considered – and an engineering perspective, where controlled smoldering is used as a tool for modifying various materials.

Smoldering fires are able to adapt to (and thus survive under) a wide range of conditions, in terms of available oxygen, stage of the fuel material, moisture and geometry. This adaptability leads to the persistency of smoldering fires. In some cases, smoldering fires are found to propagate at a steady rate under stable external conditions. In other cases, as it adapts to varying external conditions, the smoldering process may change in surprising ways. Moreover, these fires modify their own external conditions through feedback mechanisms (couplings). As an example, a change in the combustion intensity will change air currents, which in turn modify the combustion intensity. In a previous study, we found that the introduction of a cooling tube in a smoldering sample, even at a modest cooling power, led to striking temperature oscillations not otherwise observed for the experimental configuration used (Mikalsen et al., 2018). A straight smoldering front propagating along a sheet of paper in the spacing between two horizontal plates was observed to adopt a fingering form (Zik et al., 1998). The role of vertical channels for the persistence of underground coal fires was studied in an intermediate-scale experiment with one exhaust and one fresh-air channel. The chimney effect was found to *increase* with fire depth (Song et al., 2020). The complex behavior reported in these experimental studies demonstrates the limitations of approaches that assume slow and steady propagation of an active zone, which changes only slowly, if at all.

Focusing on non-steady evolution of smoldering fires, we have found it rewarding to study smoldering fires under repeated refills (addition of fuel material). We are not aware of any previous studies where such an approach has been systematically explored. This approach can be motivated in two ways. First, from a practical perspective, materials are not always fed into silos in a continuous mode, but often in batches after being processed. This refilling process involves several risks: the generation of dust clouds is one example. A not-yet-answered question is what happens if these refills are made when smoldering combustion is already ongoing. Second, through experiments with repeated refills, non-steady evolution of smoldering fires can be explored systematically. A refilling reduces abruptly the smoldering intensity, from this reduced level the intensity will again increase, but slowly. Phrased differently, the refilling takes the sample back to (towards) some low-intensity state similar to ones previously visited. This may be called a *resetting* of the smoldering sample. Thus, one obtains a series of events (mini-experiments) - that may be compared - during a single experimental run. It will be demonstrated later in this article that each refilling of fuel material represents only a partial resetting, while a complete resetting occurs after several refillings. The refilling protocol leads to extended smoldering experiments – in contrast to standard experiments on non-steady evolution, where one ignites a sample and let it burn until it self-extinguish. For each refilling, the introduction of fresh material will on one hand lower the temperature of the stored sample, while it also increases the potential for more intense combustion at a later point. We have investigated these two opposing effects experimentally in a laboratory-scale silo geometry. The time scales are well separated, the cooling leads to an almost instantaneous reduction in the combustion rate – followed by a much slower increase, in part facilitated by the additional fuel material. Focusing on the cooling phase, a master curve was obtained for the reduction in combustion rate as a function of the amount of added material.

This article is organized as follows. In Section 2, the methods used are described and discussed, including properties of the wood pellets (Section 2.1), setup and procedure used (Section 2.2), motivation for and important characteristics of the setup (Section 2.3), refilling procedure (Section 2.4), a typical experiment (Section 2.5), the data analysis used (Section 2.6), and the choice of sample sizes (sample heights) for investigation (Section 2.7). Results are given in Section 3, including an overview over the experimental data set (Section 3.1), the role of refillings in reducing the mass-loss rate (Section 3.2), and the relationship between the refilled amount of wood pellets and the change in the mass-loss rate (Section 3.3). In Section 4, the results are further discussed, including comments on the various time scales of the smoldering dynamics (Section 4.1), the difference in combustion rates before and after each refilling (Section 4.2), the question of how to scale the refilled amount of pellets (Section 4.3), regimes of the experimental curve for change in combustion rate as function of refilled mass (Section 4.4), fitting of the experimental data to a theoretical curve (Section 4.5), and an interpretation of the value that emerges from the fit in terms of the heat transfer that ensues the refill (Section 4.6). Some concluding remarks are given in Section 5.

2. Methodology

2.1. Fuel material

Wood pellets is a dominant biomass fuel, which is homogeneous, well suited for transportation, storage, and handling for example in automatic feeding assemblies for large combustion units. In the current experiments, commercial wood pellets (Hallingdal trepellets, Norway) have been used (see Table 1). The raw materials were pinewood (20%–50%) and spruce (50%–80%). Each pellet (grain) is shaped as a cylinder, with larger length than diameter in most cases. There were only small variations in the pellet diameter (8.4 ± 0.2) mm, while the length varied more (17.5 ± 5.3) mm, due to the pelleting process. These values, with the given standard deviations, were obtained from manual measurements on a population of 100 pellets (grains). The range (smallest to largest value measured) was (8.1–8.9) mm for diameter and (5.9–31.7) mm for length.

2.2. Experimental set-up and procedure

Smoldering of wood pellets has been studied in the experimental set-up shown schematically in Fig. 1. It consisted of a steel cylinder, with 15 cm diameter, surrounded by 6 cm thick thermal insulation along the side walls. This cylinder was placed on top of an aluminum plate that distributed homogeneously heat from a hotplate below it. A thin steel ladder containing 30 Type-K thermocouples was placed in the middle of the cylinder. Thermocouples were separated 2 cm vertically and 3.7 cm horizontally. Two additional thermocouples measured the temperatures on top of the aluminum plate and between the heat source and the aluminum plate, respectively. The latter was used to regulate the temperarture on top of the aluminum plate. These components were placed on a scale that registered changes in the sample mass as the experiment evolved. Temperatures and mass were recorded every 15 s.

Once the ladder was placed in the cylinder, wood pellets were slowly filled in, until the sample height reached a predetermined value. It was not possible to compact the sample further. Smoldering was initiated by switching on the hotplate for a given time (details in Section 2.3). After the hotplate had been switched off, the sample evolved independently of external disturbances, with exception of periodic refills, as described in Section 2.4.

2.3. Motivation and characteristics of set-up

Smoldering fires have been studied in the setup described in Section 2.2, which is motivated by two different considerations.

First, the setup has a silo geometry, with closed bottom and side walls. Due to the thermal insulation at the side walls, the setup mimics a much larger system in the lateral direction, since in a larger system the pellets material laterally will thermally insulate a core volume of interest. The top of the sample holder is open, which allows convectively driven exchanges of air and gases between the hot sample and the cooler laboratory atmosphere. This aspect mimic to some extent the (empty) headspace above the material in a full-scale industrial silo. Such a headspace at full scale allows convective exchanges of gas with the material in the silo during smoldering. If the sample holder had been closed, the conditions would probably have been further from the full-scale situation than they are now. This again demonstrates the difficulty in quantitative upscaling from laboratory size, which has not been attempted in the present study. Furthermore, a closed or semi-closed sample holder in the current setup could lead to issues on build-up of an explosive atmosphere, which was not a focused topic in the present work.

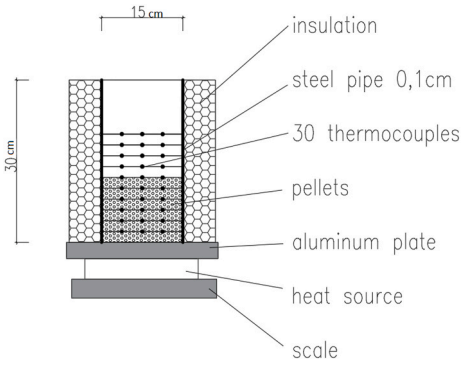

Fig. 1. Experimental set-up. Main components (top to bottom): cylindrical sample holder with wood pellets sample and positions where temperatures were measured, hotplate (aluminum plate), heat source, and scale. Further details are given in the main text.

In addition to the convective heat transfer upwards from the sample, there were conductive heat losses downwards through the aluminum plate (see Fig. 1). After the initial heating period, where the aluminum plate acted as heat source, it cooled down and became a heat sink during most of the experiment. Moreover, the convective heat loss upwards and the conductive heat loss downwards were approximately equal (Mikalsen, 2018). This is important in connection with the position vertically of the hot core in the sample, as discussed in Sections 4.4 below.

Second, the setup and procedure described in Section 2.2 have been extensively used previously. Thus, the typical behavior of smoldering in this setup is known. We have studied the relative importance of various parameters on the ignition phase (Villacorta et al., 2021), modifications of the smoldering process from a cooling loop (Mikalsen et al., 2018, 2019), modifications due to changes between quasi-opposed and quasi-forward configurations (Rebaque et al., 2020), among others. These previous studies serve as a necessary background for understanding the new experiments with repeated refillings.

Both the temperature of the hotplate (the aluminum plate below the sample, see Fig. 1) and the duration of the external heating was varied between experiments: 320 °C – 360 °C and 4.5 h–14.5 h, respectively. Typically, longer heating durations were used for larger sample size, but also for each sample size (see Section 2.7) significant variations were implemented. The main point here is that the long-run behavior during experiments with periodic refillings does not seem to be influenced by details of the initial external heating (hotplate temperature and duration). In other words, and based on our observations and results, after smoldering has been initiated, memory of the initial heating period is

Table 1
Material properties of the wood pellets used in the experiments.

C (%)	H (%)	N (%)	S (%)	Moisture (%)	Volatiles (% d.b.)	Ash (% d.b.)	Upper calorific value (kJ/kg)	Lower calorific value (kJ/kg)
47.91	6.42	0.03	0.10	6.52	82.13	0.49	18 834	17 433

Elemental composition (columns 1–4): Carbon (C), hydrogen (H), and nitrogen (N) were determined with a LECO CHN 1000 elemental analyzer, while for sulphur (S) a LECO CS230 elemental analyzer was used. Remaining fraction is predominantly oxygen.
Proximate analysis (columns 5–7): Water, ash and volatiles were determined using a Leco 701 Thermogravimetric Analyzer. The residue is char or fixed carbon. The water contents was 6.27% from this proximate analysis (performed at 105 °C). An independent measurement of the water contents was carried out with an IR-drying mass-loss measurement at 105 °C, leading to the value 6.76%. The average of these two values is given in the table.
Calorific values: (columns 8–9): Determined using bomb calorimetry (IKA C200).

soon lost.

2.4. Refilling procedure

The experimental setup and procedure described in Section 2.2 has been used in several of our previous papers, as discussed in Section 2.3. The crucial supplement to the procedure in the experiments to be reported here, is repeated refillings – additional wood pellets supplied every 8 h.

The amount of wood pellets was adjusted for each refill, so that the sample mass after refilling reached its initial value (the sample mass at the start of the experiment). Thus, the refilled amount of material varied – reflecting the combustion during the preceding 8 h period. In other words, if – during an 8-h-period – the combustion intensity and the mass-loss rate was low, only a small amount of material was added at the end of the period to reach the initial sample mass. Conversely, at the end of an 8-h-period with high mass-loss rate, a significant amount of fuel material (wood pellets) was added. All refills were done manually.

Intervals: We have also explored, in experiments not included in this article, 12-h intervals, but the use of 8-h intervals seemed to lead to a richer behavior. Refilled amount: The important aspect of our refilling scheme is that we maintain the sample approximately at constant mass. We know from previous studies with our setup that the sample size (height) influences the evolution of the smoldering process. Thus, to not introduce too many unknown factors simultaneously, we have investigated first a semi-constant mass scheme.

2.5. A typical experiment

Typical results are shown in Fig. 2, for a 14-cm-height sample, with recorded mass (part A), temperatures (part B), and temperature distribution vertically (part C). The duration of the experiment was 270 h (about 11 days). The end of the period of external heating is indicated by red, vertical lines.

The temperature measurements in Fig. 2B differed during and after the end of the external heating. During the external heating, the curves

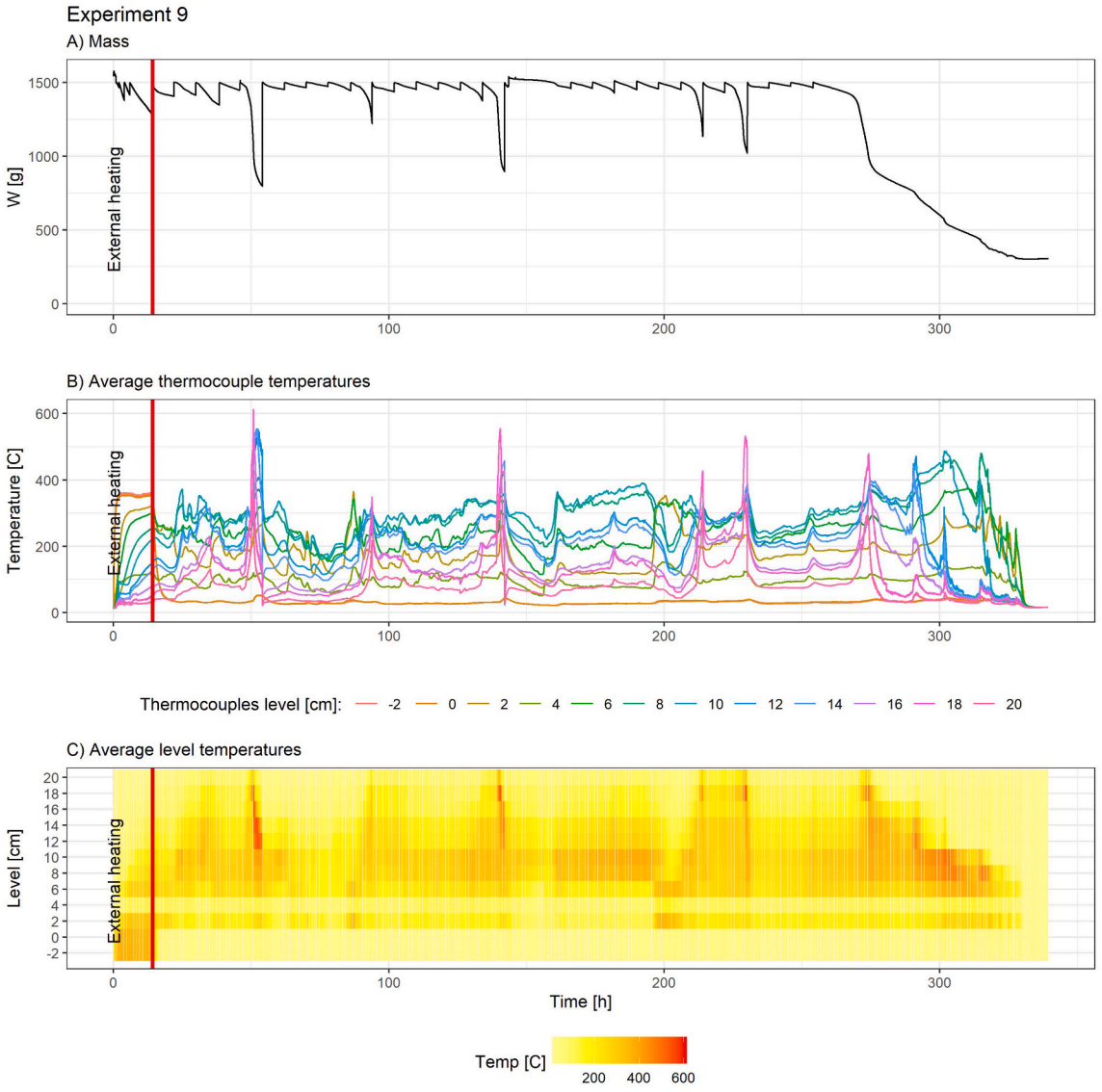

Fig. 2. A typical experiment. A: sample mass as function of time. B: temperature as functions of time - measured at positions in and above the sample (as shown in Fig. 1). Each curve (marked 2 cm–20 cm) shows the average temperature of the three thermocouples located at the same height. Temperatures measured on top of and below the aluminum plate (marked 0 cm and −2 cm, respectively) are also shown. C: temperatures recorded at the different heights as function of time. The vertical red lines indicate the time when the hotplate was switched off. (For interpretation of the references to color in this figure legend, the reader is referred to the Web version of this article.)

increased in a regular manner, with lower positions in the sample at higher temperatures. By contrast, after the hotplate had been switched off and till the end of the experiment, the temperature curves displayed a much more irregular behavior, since the smoldering process evolved freely, without any imposed heat flux. In particular, one notes short periods with particularly high temperatures, at 53 h, 140 h, and 226 h.

Focusing on the mass versus time graph in Fig. 2A, it has a characteristic saw-tooth shape, with the vertical portions corresponding to the refills, where the sample mass increased very fast. Apart from these almost instantaneous jumps in the curve, it has a negative slope, reflecting smaller or larger mass-loss rates. The mass-loss rate (the negative of the slope) changed during each 8-h period. Some 8-h periods had increasing mass-loss rate, others had decreasing rate (see also Figs. 3 and 4 below). Generally, during much of the process, the mass-loss rate was relatively low. Occasionally, however, the smoldering combustion became more intense, with a particularly steep mass curve and thus high mass-loss rate, till next refilling. An example can be found at time 53 h, where there was a much deeper dip in the mass curve than during most of the experiment. Each of these periods of intense combustion had a corresponding peak of high temperatures (Fig. 2B). Fig. 2C shows the temperature distribution along the vertical direction. For the experiment in Fig. 2, the highest temperatures were mainly in the upper half of the sample (between 6 and 12 cm), but during the intense combustion periods, high temperatures were recorded near the upper surface of the sample.

2.6. Data analysis

Statistical tools were developed to characterize the behaviour observed in the experiments. A linear prediction (Zeileis and Grothendieck, 2005) was used to estimate values in points with no recorded data (i.e., fall-outs in the data logging). Then, the mass data was smoothed to further investigate the characteristic features of the mass curve as function of time (Fig. 3), using a Local Polynomial Regression fitting (LOESS). The fitting was done locally, which means that a value in a point X_i was estimated based on the value of its neighborhood, weighted by their distance from X_i. The size of the neighborhood was controlled by the span, and the larger it was, the smoother the results were. We used a span that covered 100

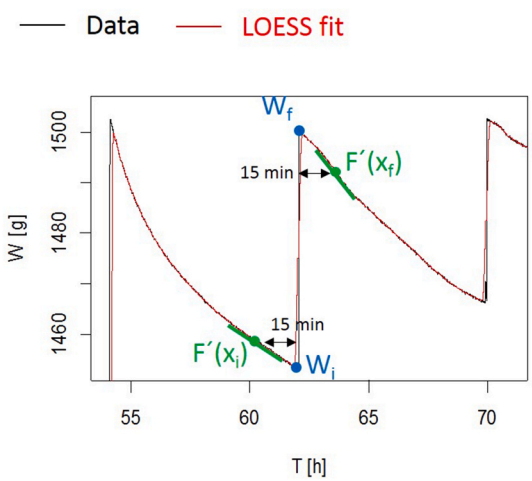

Fig. 4. Important quantities used to calculate the amount of refilled material and the combustion rate directly before and directly after the refill. See further explanation in the main text.

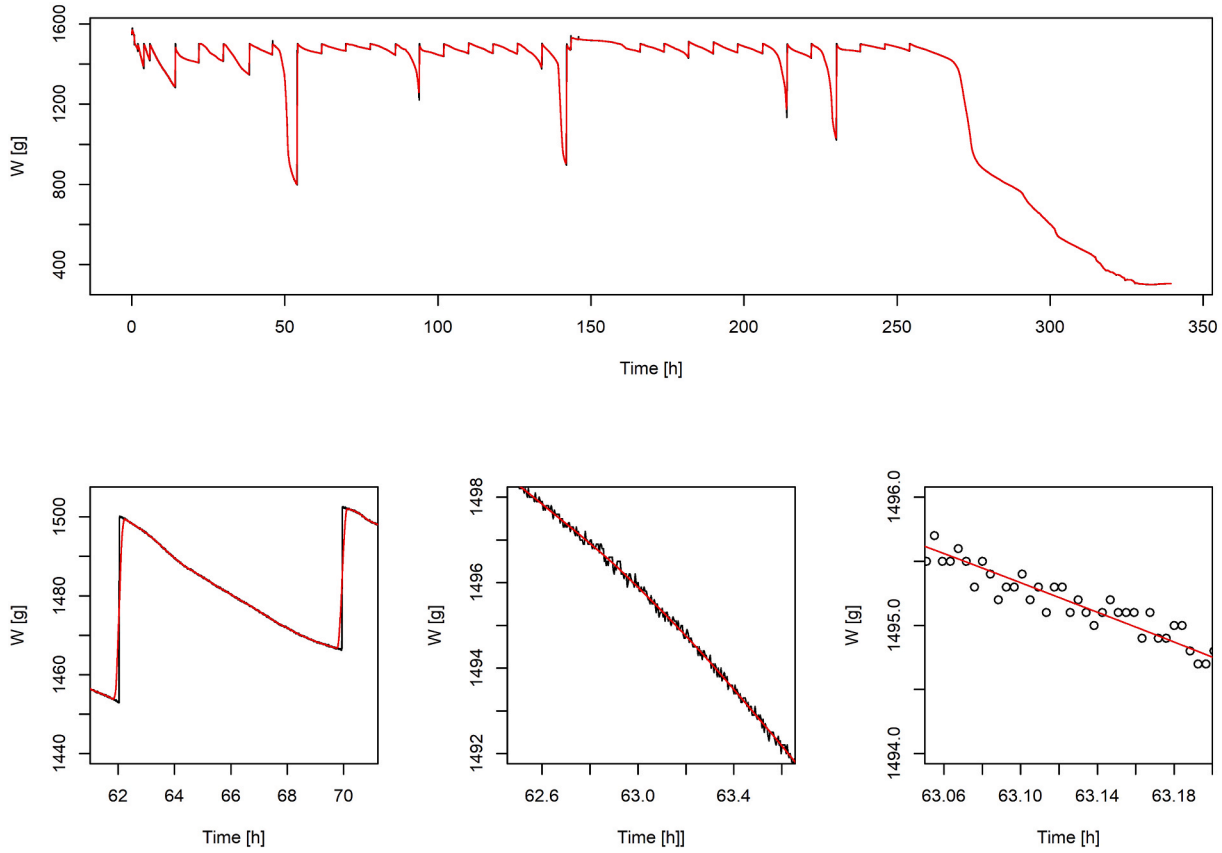

Fig. 3. Recorded sample mass (black) and curves obtained using the LOESS approach described in the main text (red). Part A shows the entire experiment, while parts B – D displays a sequence of magnifications (zooms). Note the noise in the recorded data (parts C and D). This is the same experiment as shown in Fig. 2. (For interpretation of the references to color in this figure legend, the reader is referred to the Web version of this article.)

measurements and a polynomial degree of 1.

The variation in mass was predicted using intervals of 1 s (d = 1 s), and the first derivative was calculated numerically using a centred difference approximation (Eberly 2008).

$$F'(X) = \frac{(F[x+d] - F[x-d])}{2d}$$

At each refill point (i.e., points where new material was added to take the sample back to its initial mass, see Fig. 3), the refilled mass and the difference in the combustion rates were calculated before and after refilling, defining the combustion rate (the mass-loss rate), a positive quantity, as the negative of the derivative of the sample mass curve. The refilled mass is the difference between the mass at the beginning (W_i) and at the end (W_f) of the refill (see Fig. 4), while the difference in the combustion rates was obtained from the first derivative of the adjusted curve (i.e., LOESS prediction) 15 min before (CR_i) and 15 min after (CR_f) the refilling point. The 15-min interval was chosen because the smoothed curve does not fit well near the refilling point (compare red and black in vertical parts of the curve in Fig. 3B). In addition, the 15-min interval allowed the system to stabilize after the disturbance from the refill. All these quantities are displayed in Fig. 4.

2.7. Choice of sample sizes

Based on experience from previous studies using the setup described above, we decided to restrict the experiments with refills to a few values of the sample size (through the initial sample height).

First, there seemed to be a lower threshold for inducing self-sustained smoldering using the protocol described above, at a sample height of 6 cm (Villacorta et al., 2021). Since the present experiments with refills were aimed at long duration, it was important to avoid conditions that too easily led to self-extinguishment. It was therefore decided to stay well above the border case of 6 cm and use as lowest value a sample height 10 cm. Samples with heights 10, 12, 14, 16, and 20 cm have been explored, but only results for sample heights 10, 12, and 14 cm will be reported below. We observed that for heights 10, 12, and 14 cm, smoldering occurred in a way that resembled previous experiments without refilling.

Different behavior was observed in the runs with 16 and 20 cm height: 16-cm-height samples did not display self-sustained smoldering, but self-extinguished as the period with external heating ended (4 experiments). Due to the low number of 16-cm experiments, it is unclear if this is a statistical variation or reflects fundamental underlying behavior. The issue has not been further pursued. As for 20-cm samples, self-sustained smoldering was observed, but the behavior differed from previous experiments without refills and the experiments at height 10, 12, and 14 cm reported below; temperatures were relatively low, and – most important – short periods with high temperatures and high mass-loss rate (as in Fig. 2) did not emerge. Interestingly, for 20-cm samples we have discovered voids when remaining material was removed after the experiment. Under field conditions, such voids indicate smoldering of limited spatial extent that has self-extinguish. Possibly, these observations for sample heights 16 and 20 cm suggest that one – for these sample sizes - is moving into a regime where the sample becomes large compared with the size of the active zone.

3. Results

3.1. Overview of experiments

In this article, we report results from 17 experimental runs, carried out and analysed as described in Section 2. Together, these experiments represent 2246 h (about 93 days) run-time (813 h with sample height 10 cm, 900 h with 12 cm, and 533 h with 14 cm). The duration of the experiments varied significantly, from 30 h (about 1 day) to 470 h (about 20 days). Experiments that self-extinguished had relatively short duration (30 h–125 h), while experiments that terminated through stoppage in refillings had longer duration (120 h–470 h). For each experimental run, the duration was determined as the time from the start of the external heating till the last refilling, thus excluding the final burn-out phase (stoppage in refillings) or decay phase (self-extinguishment).

3.2. Refills lead to reduced mass-loss rate

The main consequence of refillings was that the sample was cooled. Reduced temperatures led to a lower mass-loss rate (i.e., a reduced slope in the mass curve). For each refill, the mass of the added wood pellets and the change in mass-loss rate should be systematically related. This covariation is the focus of the analysis that follows below. As an introduction, the covariation for the experiment in Figs. 2 and 3 is displayed in Fig. 5. On the long view, refills lead to more fuel material being available for combustion later. Thus, extended experiments are possible, which was part of our aim with this study.

Following the procedure described in Section 2.6, we analysed each peak of the mass-as-function-of-time curve (each refill), as shown in Fig. 5A, where the refills are marked with consecutive numbers from 1 to 28. The points in part B have the same numbering. In this plot, the horizontal axis shows the size of the refill (the amount of wood pellets refilled), which was found from the length of the vertical part of the mass curve for each refill (Fig. 5A). As an example, for refill 10, one can read off in the upper part of the figure that the mass changed from approximately 1280 g–1500 g. As fraction of the initial mass, this is (1500 g–1280 g)/1500 g = 0.19, which is the position of point 10 along the horizontal axis. On the vertical axis in Fig. 5B, we plot the difference in combustion rates (mass-loss rates), from slightly before till slightly after the refill. For refill 10, it is evident in Fig. 5A that the mass curve is much steeper before this particular refill than after, and therefore the mass-loss rate before refill is much larger than after, leading to a large difference (mass-loss rate before refill minus mass-loss rate after), as shown. Thus, Fig. 5B gives the difference in combustion rate as function of the refilled mass.

For small refills, the change in combustion rate (mass-loss rate) is small, but it increases for large refills. More surprisingly, for the largest refills, the change in combustion rate is again close to zero. An example is refill 5, the largest one. It will be demonstrated below that the curve shape suggested by the points in Fig. 5B holds for the entire data set. For increasing refill, there are first low values for the difference in combustion rate, followed by a rapid increase towards a peak, and finally a fall-off towards low values.

3.3. Refill versus change in mass-loss rate

Repeating this analysis for all experiments, results followed a similar trend for all sample heights, as shown in Fig. 6. Three quantities are displayed as function of refilled amount of wood pellets (as fraction of initial sample mass). Part A shows the combustion rate before the refill; part B the combustion rate after the refill; and part C the difference in the combustion rate from before till after the refill. The data is in general noisy, this is not noise in the measurement but reflect the stochastic character of smoldering processes. In particular, part of the data at low values of the refill (refills 0–5% in parts A and B and 0–10% in part C), can experimentally hardly be distinguished from ordinate value 0. Since the data is noisy, A LOESS fit (span = 0.25, and degree = 2) was used for plotting trends in the data for each sample height (colored lines).

Below, similarities and differences between Fig. 6A and B will be discussed (Section 4.2), the scaling implied by using refills measured in percentage of initial mass instead of mass (in grams) (Section 4.3), and the curve shape in the three graphs, with the four regimes indicated in Fig. 6 (Section 4.4).

The data in Fig. 6C is replotted in Fig. 7. The difference in combustion rate (mass-loss rate) is still along the vertical axis, while along the

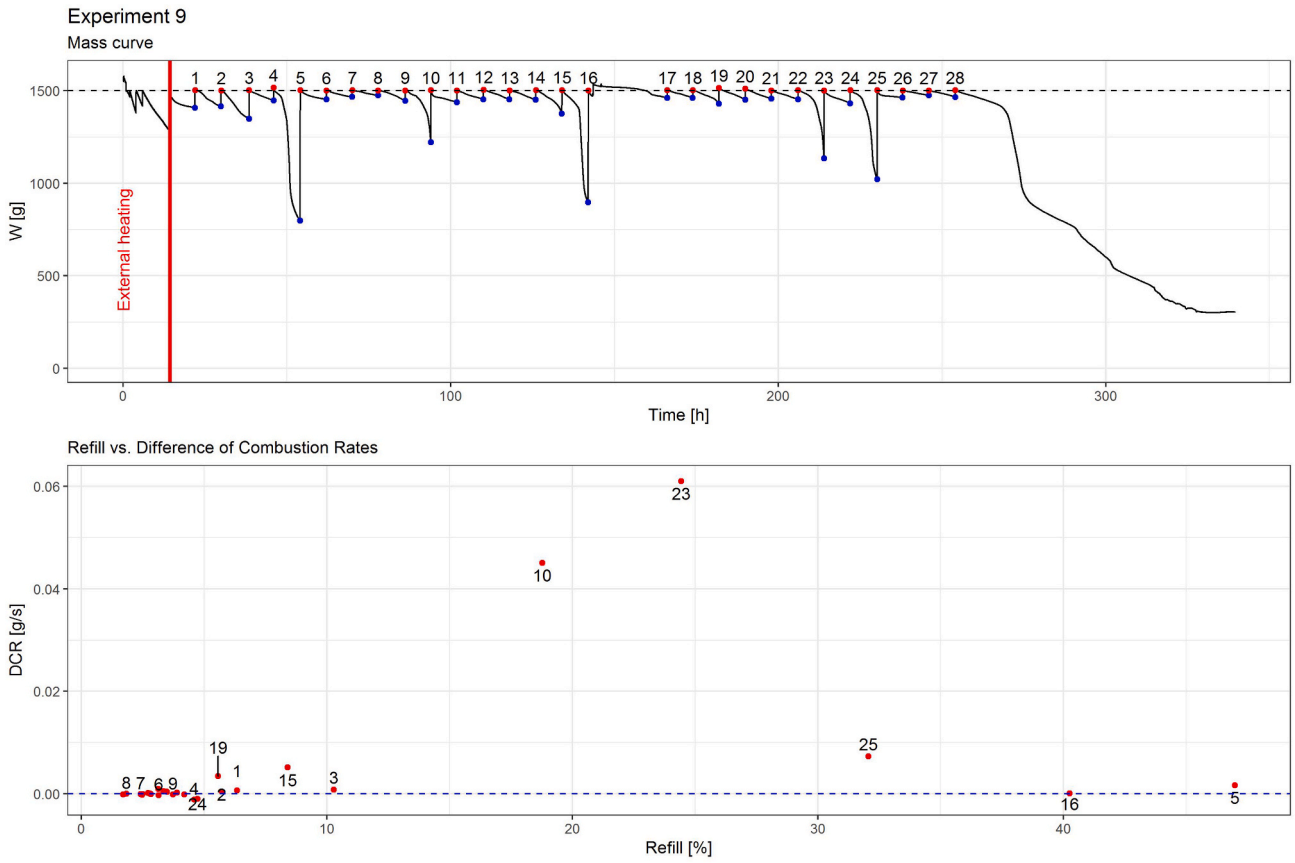

Fig. 5. Results from analysing the same experiment as shown in Figs. 2 and 3. Part A: smoothed mass data, with refills numbered. The analysis has been carried out from the red vertical line on. Thus, the initial period with external heating (hotplate on) has been excluded from the analysis. Part B: results, in terms of the difference in combustion rate (DCR) (mass-loss rate) from directly before to directly after the refill – as a function of the refilled amount of wood pellets (as fraction of initial sample mass). (For interpretation of the references to color in this figure legend, the reader is referred to the Web version of this article.)

horizontal axis, the combustion rate before each refill is shown. The plotting symbols indicate regimes as defined in Fig. 6. The close-up (zoom) in Fig. 7b again demonstrates that the lowest values of the change in combustion rate cannot be distinguished from the noise around value zero.

4. Discussion

4.1. Relevant time scales

The experiments reported in this manuscript can be viewed from several perspectives, corresponding to different time scales. The shortest time scales are connected to inherent variations in the smoldering process. In this study, we have imposed a time scale corresponding to 8-h-interval refills. The main analysis in this work is connected to the 8-h time scale, where a statistical description of the refills as unconnected events is presented. This approach was described in Section 3 and will be further discussed below.

There is, however, also structure in the results at longer time scales, see Fig. 5A. This structure emerges through the sequence of refillings. It is clear from Fig. 5A, and the other experiments, that the refilled amounts do not come in a random sequence. Instead, there seems to be a systematic evolution in the refill size. An example is the refills 10–16 in Fig. 5A. Here, the refilled amount first decreases (refills 10–12) and then increases (refills 12–16). This is a typical evolution that is often observed between two large or intermediate-size refills. In some experiments such a pattern is repeated in an almost periodic manner, in others a more irregular pattern is observed. We will return to the evolution over several 8-h intervals in a separate publication.

The evolution during sequences of 8-h intervals has some further implications. A priori, one may have guessed that each refill would take the smoldering process back to the same stage, so that approximately the same evolution occurred during each 8-h interval, leading to a series of mini-experiments that could be directly compared. Such a conceivable situation could be termed a regularization of the smoldering process. The results demonstrate that such a complete regularization at the 8-h time scale does not take place. However, regularization does occur at a longer time scale, typically with a large or intermediate-size refilling as terminus. On regularization, see also Section 4.2.

4.2. Combustion rates before and after refill

Both the combustion rate before the refill (Fig. 6A) and the combustion rate after the refill (Fig. 6B) display a peak around 20% refill. The peak is much higher in part A, which is reasonable, the refilling leads to cooling, and lower temperatures leads to lower combustion rate (mass-loss rate). However, it is worth noting that there still is a weak peak structure in part B. This means that for the cases around the peak in part B, the refill did not supply sufficient cooling to eliminate all traces of a high combustion rate before the refill. Thus, the sample has only to a certain degree been reset by the refills. A complete resetting would have led to the same combustion rate in all cases (for all values of the refilled amount), i.e., a horizontal curve in Fig. 6B. See also Section 4.1, last paragraph.

4.3. Scaling of the refilled amount

The amount of wood pellets used in each refilling, is in Fig. 6 given as

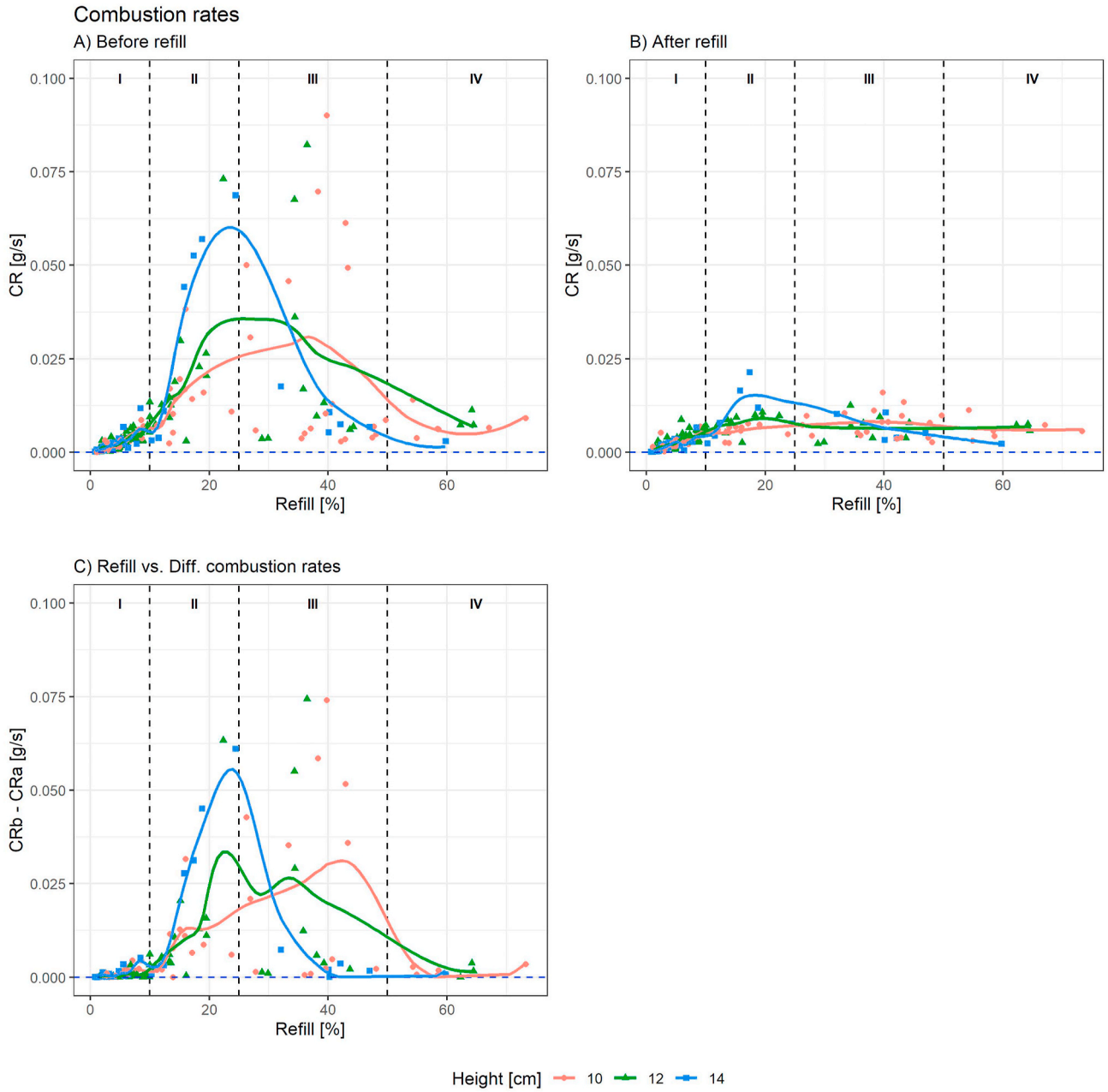

Fig. 6. Combustion rates (CR) as functions of refilled amount of pellets, for all refills in the experimental data set (all experiments). The refilled amount (refilled mass) is given as fraction of the initial sample mass. Points are experimental data, trend lines were obtained as explained in the main text. Both points and lines are color coded according to sample size. Part A: Combustion rates before refill, Part B: Combustion rates after refill, Part C: Difference in combustion rate, thus, data in part A, with data in part B subtracted (i.e., combustion rate before refill (CRb) minus combustion rate after refill (CRa)). (For interpretation of the references to color in this figure legend, the reader is referred to the Web version of this article.)

fraction of the initial mass. In other words, the refilled amount is rescaled by the initial sample mass. Fig. 6A indicates that this is a reasonable scaling, since the peak for the three explored sample sizes are close. The scaling is not perfect, and one may argue that a better fit could be obtained with an adjusted scaling. However, the data is noisy, and a more sophisticated scaling should have some theoretical motivation.

For the difference in combustion rate in Fig. 6C, the scaling is less convincing. However, the data here has more noise, a result of the fact that they emerge by subtracting one noisy data set (Fig. 6B) from another one (Fig. 6A).

4.4. Four regimes

The curves in Fig. 6 may divided into four regimes, as indicated by vertical lines in the figure.

Regime I: Up to 10% refill (refilled mass up to 10% of initial mass): the combustion rates before refills increase linearly (Fig. 6A), and the refill did not affect it, since the combustion rate after refill also increases linearly with refill and is of the same size (Fig. 6B). As consequence, the difference in the combustion rates is close to 0 (Fig. 6C). Thus, the refills in this regime did not influence the smoldering process.

Regime II: From approx. 10%–25% refills: there is a rapid increase in the combustion rate before refill, which was halted when more fuel material was added (combustion rates after refill were much lower). In

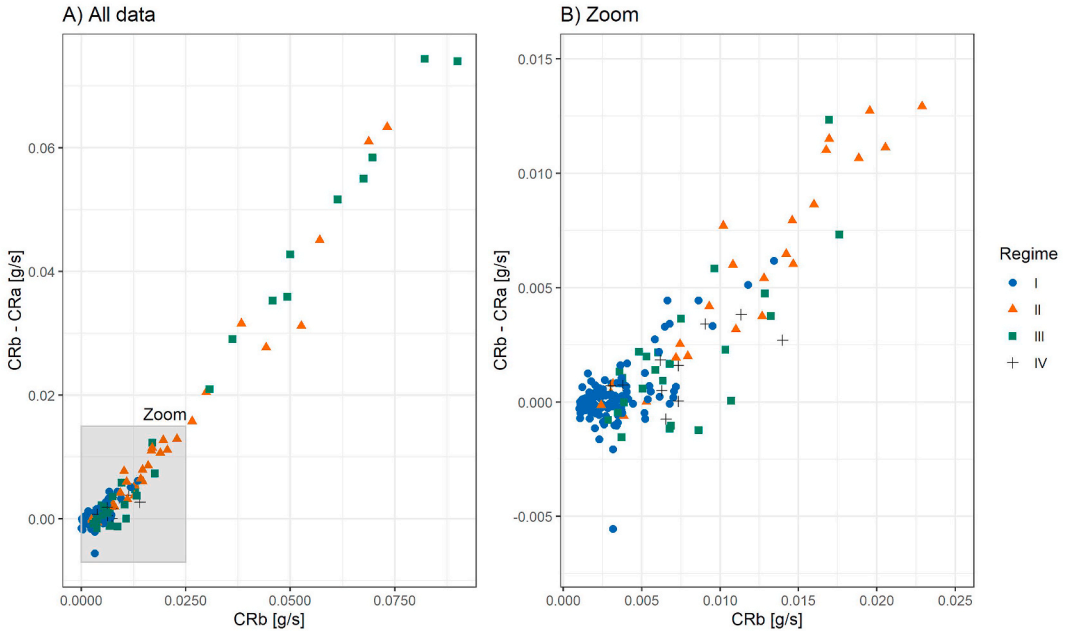

Fig. 7. The data in Fig. 6C as function of the combustion rate before refill (CRb). Part A shows the full data set, while the grey region in part A is shown in close-up (zoom) in part B. Plotting symbols indicate regions as specified in Fig. 6.

this regime, the smoldering processes were more intense and occurred at higher temperatures. Consequently, the mass loss was larger and so was the refilled amount of wood pellets. A large refill leads to a stronger cooling of the sample and a larger reduction in the combustion rate. The nonlinear curve shapes in Fig. 6, parts A and C are reasonable in view of the highly nonlinear dependency of the combustion rate on temperature (Arrhenius expression). This point will be discussed in more detail below.

Regime III: From 25% to 50% refills: the combustion rates before refills level off and start to decrease. In this regime, the large refilled amounts of wood pellets indicate a relatively long period of intense (high temperature) smoldering prior to the refill. During this period, the sample lost significant amounts of heat through strong convection and radiation, leading to reduced temperatures. Thus, the cooling effect of the added material is less pronounced.

Regime IV: Refills higher than 50%: the combustion rate before refills was low and similar to the values after refills (i.e., differences were close to 0). In this regime, the sample had lost heat to an even larger extent than in the previous regime. The added fuel material, when the refill finally occurred, had close to no cooling effect.

Referring to Fig. 5, the regimes are reflected in differences in the shape of the mass curve prior to the refill. Refills 10 and 23 belong to regime II, and the (negative) slope of the mass curve (and thus the mass-loss rate) increases all the way till the refill. On the other hand, refills 16 and 25 belong to regime III. For these refills, the slope of the mass curve decreases the last hours before the refill, as result of significant heat losses. This is even more pronounced for refill 5, on the border to regime IV.

The particularly large heat losses when the mass-loss rate is high (in regimes III and IV) have to do with the position of the hottest part of the sample, as shown in Fig. 2C. During most of the experiment, the hottest part is well below the surface of the sample, in the upper half of the sample, where it is thermally shielded but still has sufficient access to oxygen. However, Fig. 2C also shows that during the most intense combustion periods, the hottest part of the sample is near or at the upper surface of the sample. Here, there is abundant access to oxygen, which makes possible the intense combustion. However, the heat losses upwards (radiation and convection) are also much larger. Eventually, this leads to reduced temperatures at the sample surface, and thus reduced mass-loss rate, reflected in a less steep mass curve.

These variations are displayed under a different perspective in Fig. 7. Regimes I and IV are concentrated near the origin, thus, for both these regimes, the combustion rate before refill and the change in combustion rate as result of the refill are both small. However, the cause is quite different. In regime I, the combustion rate (mass-loss rate) was low during the preceding 8-h period, leading to a small refill, that can only change the combustion rate little, if at all. In regime IV, on the other hand, the mass loss during the 8-h period leading up to the refill had been significant, and therefore a significant amount of wood pellets was refilled. Such a refill could potentially cool the sample much. However, in these cases, there had already been a large heat loss from the sample through convection and radiation (since the hottest part of the sample was at or near the upper surface of the sample), and the mass-loss rate just prior to the refill was low (leading to low values for CRb). Therefore, the large refill can hardly cool the sample further (leading to low values for (CRb – CRa)).

Regimes II and III have data points in Fig. 7 that extend to high values for both CRb and (CRb – CRa). The mass loss prior to the refill was large, but not as large as for regime IV (since the hottest part of the sample was lower that for regime IV). The sample had not experienced strong cooling through radiation and convection, as for regime IV. Thus, a large amount of cold wood pellets hit a still hot sample, leading to a considerable cooling (large value for (CRa – CRb)). Regimes II and III correspond to the peak in Fig. 6.

The data set in Fig. 7A is approximately linear, but a closer inspection reveals a slight arching.

4.5. *Quantitative treatment of regime II*

One may ask if it is possible to understand the curve shape in Fig. 6C quantitatively and if useful information can be extracted from the data. Here, regimes III and IV are challenging, since they are dominated by radiative and convective heat losses in the upward direction, as discuss in Section 4.3. These heat losses define the stage of the smoldering at the time of the refill, but they are not easy to model. Regimes I and II probably represent the same functional relationship between refilled amount and change in mass-loss rate. However, the signal-to-noise ratio in Regime I is clearly unfavorable for quantitative analysis.

This leaves us with Regime II, which has a simple non-linear increase. Considering the Arrhenius equation, such a functional relationship seems reasonable. According to the Arrhenius equation, the local mass-loss rate depends on the local temperature through $A_0 \cdot e^{-\frac{E_a}{RT}}$, where A_0 represents the pre-exponential factor, E_a the activation energy, both of them material-specific parameters, R is the ideal gas constant and T the absolute temperature (the expression must be multiplied by the mass of the relevant volume to give physical mass-loss rate in g/s). Through this equation, the mass-loss rates just before and after each refilling can be calculated from the measured temperatures at these times. On the other hand, the sample mass is recorded throughout each experiment, independently of the temperature measurements. In the analysis below, data from these two sources will be combined. Specifically, characteristic temperatures before and after each refill – and the refilled amount of wood pellets will be considered.

To obtain mass-loss rates from measured temperatures, the sample should in principle be divided into a large number of cells and the Arrhenius equation applied for each of them. However, the success of such an approach is uncertain, since temperatures are only measured at some positions in the sample. Therefore, a more indirect method with an approximation (a model) for heat generation and heat transfer has been chosen. The average value of the four highest temperatures measured in the sample the moment before (T_b) and after (T_a) the refilling were used to express the mass-loss rate. Since the mass-loss rate (combustion rate) increases rapidly with temperature (see Arrhenius expression above), the hottest parts of the sample dominate the heat production.

Over the short times considered in this study (from refill to the point 15 min later, see Fig. 4), the effect of the refilling is to cool the sample. As a simplified heat-transfer mechanism, it can be assumed that only the hot core (the hottest part of the sample) will be cooled. As explained above (see also Fig. 2C), this hot core is in the upper half of the sample for the intermediate-size refillings we consider here (regime II). We further assume that the hot core experiences a temperature reduction that is proportional to the refilled mass following Equation (1).

$$T_b - T_a = C \cdot \Delta m \tag{1}$$

Here, C is a constant and Δm is the added mass. The temperatures T_a and T_b were calculated from the data for each refilling. Equation (1) gives a connection between measured temperatures and measured refilled mass for each refill, where the value of the constant C remains to be determined.

From temperatures T_a and T_b and the Arrhenius equation, expressions for the mass-loss rate can be found. The Arrhenius equation contains two material-specific parameters, the activation energy E_a and the pre-exponential factor A_0. The pre-exponential factor is difficult to determine accurately. Therefore, we consider the ratio of mass-loss rates just before and after the refilling, instead of the difference between the rates as for Fig. 6.

$$\frac{A_0 \cdot e^{-\frac{E_a}{RT_a}}}{A_0 \cdot e^{-\frac{E_a}{RT_b}}} = e^{-\frac{E_a}{RT_a} - \left(-\frac{E_a}{RT_b}\right)} = e^{\frac{E_a}{R}\left(\frac{1}{T_b} - \frac{1}{T_a}\right)} = e^{\frac{E_a}{R}\left(\frac{T_a - T_b}{T_a \cdot T_b}\right)} = e^{-\frac{E_a}{R}\left(\frac{C \cdot \Delta m}{T_a \cdot T_b}\right)} \tag{2}$$

Equation (1) was used in the final step. Note that the final expression does not depend on the pre-exponential factor.

The ratio of combustion rates $\frac{CR_a}{CR_b}$ (left-hand side of Equation (2)) is modelled based on $\frac{\Delta m}{T_a \cdot T_b}$ (from the exponent at the right-hand side of Equation (2)) for regime II, fitting a log-normal linear model as follows and shown in Fig. 8:

$$ln\left(\frac{CR_a}{CR_b}\right) = -\beta\left(\frac{\Delta m}{T_a \cdot T_b}\right) \tag{3}$$

Here, $\beta = \frac{E_a \cdot C}{R}$; R the gas constant (R = 8.3145 J/(mol K)), E_a the activation energy (E_a = 91 400 J mol^{-1}) (Villacorta et al., 2021), and C the constant to be estimated.

4.6. Interpretation of the C-value

The data fitting in Equation (3) and Fig. 8 gives as outcome the value for the constant C as C = 0.15 K/g. If the value is reasonable, this can be taken as support for the two main assumptions made in Section 4.5:

First, it was assumed that it is possible to obtain a reasonable estimate for the heat production in the sample by applying the Arrhenius equation only to the hottest part of the sample and neglecting all other parts. Second, it was assumed that only the hottest part of the sample is cooled by the refilled material, and that the simple, linear expression in Equation (1) describes the cooling. More precisely, we assume that thermal equilibrium is not at all reached during the short time considered here, and that all heat exchange occurs between the hot core of the sample and the cold refilled material.

To evaluate the assumptions, a more quantitative description of the heat exchange between the hot core and the cold refilled material is needed. The amount of heat removed from the hot core is $\rho \cdot V_{core} \cdot c_v \cdot (T_b - T_a)$, where ρ is the density of the pellets, V_{core} the volume of the hot core and c_v the heat capacity of the wood pellets. Similarly, the amount of

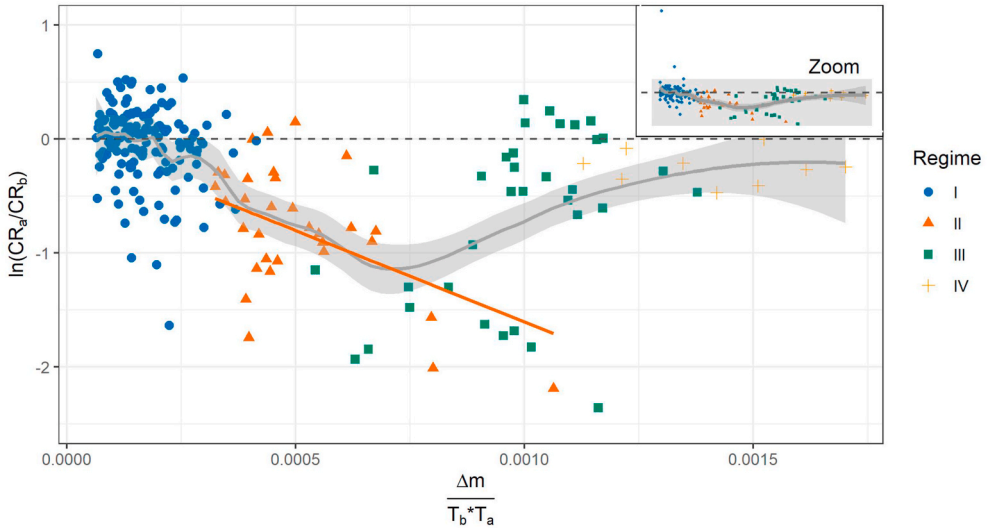

Fig. 8. Log-normal linear fitting for regime II (orange/red triangles). Further details in the main text. (For interpretation of the references to color in this figure legend, the reader is referred to the Web version of this article.)

heat received by the refilled material is $\rho \cdot V_{new} \cdot c_v \cdot \Delta T$, where V_{new} is the added (refilled) volume and ΔT its temperature increase. These two amounts of heat must be equal. Introducing: $\rho \cdot V_{new} = \Delta m = \frac{T_b - T_a}{C}$ (where Equation (1) was used) one obtains for the temperature increase in the newly added material $\Delta T = C \cdot \rho \cdot V_{core}$. The heat capacity was cancelled.

The density of the wood pellets (as packed) was 1020 kg/m^3 (Villacorta et al., 2021). As for the hot core, it typically does not extend across the entire cross section of the sample. This is probably due to convective air currents that extend down into the sample. These air currents are discussed at length in (Villacorta et al., 2021). The typical shape of a hot core that contains four measurement points is pairs of points at two height levels, one pair directly above the other. With such a typical shape, the hot core extends over a vertical distance 4 cm and covers two thirds of the cross section, which gives $V_{core} \approx 470\ cm^3$. The temperature increase can then be obtained:

$$\Delta T = C \cdot \rho \cdot V_{core} = 0.15\ K/g \cdot 1.02 g/cm^3 \cdot 470\ cm^3 \approx 70\ K \quad (4)$$

This value for the (short-term) temperature increase from room temperature for the newly added material is reasonable. This fact supports the analysis above. Building on the Arrhenius expression and simplifying the heat transfer directly after a refill, we arrived at a consistent description of our data.

5. Conclusions

Storage of biomass as wood pellets is and will continue being key in a renewable-energy future. To secure the availability of these materials, safe storage systems should be ensured. Self-heating, self-ignition and smoldering combustion in silos have previously been widely studied due to high frequency of occurrence. A specific situation is refilling of these silos when a smoldering process is already ongoing. This process has been studied by experiments at different sample heights (10, 12 and 14 cm) in a 15 cm diameter silo, and the influence of the refill size was studied. If the refill is small or large, it does not influence the behaviour of the smoldering fire, and the same combustion rate was observed before and after the refill. However, if the refill is intermediate in size, the smoldering process is normally ongoing under a relatively high combustion rate, and by refilling the laboratory-scale silo, these rates decrease, slowing down the combustion process (Fig. 6). For one of the regimes, we have given a consistent quantitative description of the data (Sections 4.5 and 4.6).

A (reasonable) assumption made above is that added cold material - to first approximation and on short time scales - leads to cooling of the hot core of the sample only. Conceptually, this may be transferred to industrial scale. Adding cold material on top of a silo or waste dump with an ongoing smoldering fire could lead to temperature reduction primarily in its hottest (and most dangerous) parts. This will not extinguish the smoldering fire, but it could give more time to fight the fire through other means.

Author contributions

Nieves Fernandez-Anez: Data Formal analysis and Interpretation, Writing – original draft, Writing – review & editing, Anita Katharina Meyer: Experiments, Writing – review & editing, Javier Elio Medina: Data Formal analysis and Interpretation, Writing – review & editing, Gisle Kleppe: Data Formal analysis and Interpretation, Writing – review & editing, Bjarne Christian Hagen: Conceptualization, Writing – review & editing, Vidar Frette: Conceptualization, Experiments, Writing – review & editing, All authors have read and agreed to the published version of the manuscript.

Declaration of competing interest

The authors declare that they have no known competing financial interests or personal relationships that could have appeared to influence the work reported in this paper.

Acknowledgements

The authors gratefully acknowledge funding from the Research Council of Norway, project 238329: Emerging Risks from Smoldering Fires (EMRIS). The authors would also like to thank Sofie Hagen for assisting with the measurements of pellet size – and Christoph Wanke for help with the measurements of material properties, and for enjoyable interaction throughout the EMRIS prosject.

References

Babrauskas, V., 2003. Ignition Handbook : Principles and Applications to Fire Safety Engineering, Fire Investigation, Risk Management and Forensic Science. Fire Science Publishers/SFPE, Issaquah, WA.
Bluvshtein, N., Villacorta, E., Li, C., Hagen, B.C., Frette, V., Rudich, Y., 2020. Early detection of smoldering in silos: organic material emissions as precursors. Fire Saf. J. 114, 103009. https://doi.org/10.1016/j.firesaf.2020.103009.
Eberly, D., 2008. Derivative Approximation by Finite Differences. Magic Software, Inc.
Gentilhomme, O., Truchot, B., Verdier, F., Poichotte, F., Barrier-Guillot, B., 2019. Experimental investigation of a smouldering fire in an under-ventilated silo. Process Saf. Prog. 38, e12012 https://doi.org/10.1002/prs.12012.
Guo, W., 2013. Self-heating and Spontaneous Combustion of Wood Pellets during Storage. University of British Columbia.
Hedlund, F.H., 2018. Carbon dioxide not suitable for extinguishment of smouldering silo fires: static electricity may cause silo explosion. Biomass Bioenergy 108, 113–119. https://doi.org/10.1016/j.biombioe.2017.11.009.
Krause, U. (Ed.), 2009. Fires in Silos, Hazards, Prevention and Fire Fighting. WILEY-VCH Verlag GmbH & Co. KGaA, Weinheim.
Larsson, S.H., Lestander, T.A., Crompton, D., Melin, S., Sokhansanj, S., 2012. Temperature patterns in large scale wood pellet silo storage. Appl. Energy 92, 322–327. https://doi.org/10.1016/j.apenergy.2011.11.012.
Lohrer, C., Krause, U., Steinbach, J., 2005. Self-ignition of combustible bulk materials under various ambient conditions. Process Saf. Environ. Protect. 83, 145–150.
Madsen, D., Azeem, H.A., Sandahl, M., van Hees, P., 2018. Levoglucosan as a tracer for smouldering fire. Fire Technol. 54, 1871–1885. https://doi.org/10.1007/s10694-018-0773-4.
Mikalsen, R.F., 2018. Fighting Flameless Fires. Doctoral Thesis. University of Magdeburg, Germany.
Mikalsen, R.F., Hagen, B.C., Frette, V., 2018. Synchronized smoldering combustion. EPL (Europhysics Letters) 121, 50002. https://doi.org/10.1209/0295-5075/121/50002.
Mikalsen, R.F., Hagen, B.C., Steen-Hansen, A., Krause, U., Frette, V., 2019. Extinguishing smoldering fires in wood pellets with water cooling: an experimental study. Fire Technol. 55, 257–284. https://doi.org/10.1007/s10694-018-0789-9.
Moreno, V.C., Cozzani, V., 2015. Major accident hazard in bioenergy production. J. Loss Prev. Process. Ind. 35, 135–144. https://doi.org/10.1016/j.jlp.2015.04.004.
Ogle, R.A., Dillon, S.E., Fecke, M., 2014. Explosion from a smoldering silo fire. Process Saf. Prog. 33, 94–103. https://doi.org/10.1002/prs.11628.
Ohlemiller, T., 1985. Modeling of smoldering combustion propagation. Prog. Energy Combust. Sci. 11, 277–310.
Rein, G., 2016. Smoldering combustion. In: SFPE Handbook of Fire Protection Engineering, pp. 581–603. https://doi.org/10.1007/978-1-4939-2565-0_19.
Rebaque, R., Ertesvåg, I.S., Mikalsen, R.F., Steen-Hansen, A., 2020. Experimental study of smouldering in wood pellets with and without air draft. Fuel 264, 116806. https://doi.org/10.1016/j.fuel.2019.116806.
Russo, P., De Rosa, A., Mazzaro, M., 2017. Silo explosion from smoldering combustion: a case study. Can. J. Chem. Eng. 95, 1721–1729. https://doi.org/10.1002/cjce.22815.
Searchinger, T.D., Beringer, T., Holtsmark, B., Kammen, D.M., Lambin, E.F., Lucht, W., Raven, P., van Ypersele, J.P., 2018. Europe's renewable energy directive poised to harm global forests. Nat. Commun. 9, 10–13. https://doi.org/10.1038/s41467-018-06175-4.
Song, Z., Huang, X., Kuenzer, C., Zhu, H., Jiang, J., Pan, X., Zhong, X., 2020. Chimney effect induced by smoldering fire in a U-shaped porous channel: a governing mechanism of the persistent underground coal fires. Process Saf. Environ. Protect. 136, 136–147. https://doi.org/10.1016/j.psep.2020.01.029.
The European Commission's Knowledge Centre for Bioeconomy, 2019. Brief on Biomass for Energy in the European Union.
Torero, J.L., Gerhard, J.I., Martins, M.F., Zanoni, M.A.B., Rashwan, T.L., Brown, J.K., 2020. Processes defining smouldering combustion: integrated review and synthesis. Prog. Energy Combust. Sci. 81, 100869. https://doi.org/10.1016/j.pecs.2020.100869.
Villacorta, E., Haraldseid, I., Mikalsen, R.F., Hagen, B.C., Erland, S., Kleppe, G., Krause, U., Frette, V., 2021. Onset of smoldering fires in storage silos: susceptibility to design, scenario, and material parameters. Fuel 284, 118964. https://doi.org/10.1016/j.fuel.2020.118964.
Zeileis, A., Grothendieck, G., 2005. Zoo: S3 Infrastructure for Regular and Irregular Time Series. ArXiv Preprint Math/0505527.
Zik, O., Olami, Z., Moses, E., 1998. Fingering instability in combustion. Phys. Rev. Lett. 81, 3868–3871. https://doi.org/10.1103/PhysRevLett.81.3868.